

A Proposal:

Volatile Ice Rheology Laboratory Facility

at NASA Ames Research Center

Moffett Field, CA 94305

NASA-ARC Personnel (*title/role, and additional affiliation if applicable*)

Orkan Umurhan (Scientist-PI, SETI Institute),
Jeffrey M. Moore (Scientist),
Arwen Dave (Engineer, Millennium Engineering),
Emmett Quigley (Engineer Technician),
Nicholas Scott (Scientist/Engineer, BAER)
Bryson Rogers (Engineering Technician Apprentice, KISS Engineering)
Carrie Chavez (Lab Technician)

Draft Date: December 12, 2017

TABLE OF CONTENTS

Volatile Ice Rheology Laboratory Facility, NASA ARC

INTRODUCTION	2
VOLATILE ICE RHEOLOGY	3
EXAMPLES FROM AROUND THE OUTER SOLAR SYSTEM	7
1. Glacial flow of volatile ices (Pluto)	7
2. Bladed Terrain (Pluto)	8
3. Geysers and Plumes (Triton)	8
VIC (VOLATILE ICE CRUSHER) PROPOSED EXPERIMENTAL APPARATUS	9
1. Experimental approach and previous design	9
2. Volatile Ice Crusher (VIC)	11
3. Typical Experimental Procedure	14
4. Measurements: time estimates and bootstrapping technique	15
• Extended Use	17
2-5-8-10 YEAR GOALS	17
PROPOSED COSTS OF A PROTOTYPE AND PERSONEL ROLES	19
REFERENCES	22
APPENDIX: A DETAILING OF LIST OF MATERIAL/LABOR COSTS	23

INTRODUCTION:

Planetary bodies of the outer solar system, including satellites of the gas giants, dwarf planets, comets and Kuiper belt objects, harbor surface ices made of volatile molecules like N₂, CO, CH₄, C₂H₆, CH₄-clathrates, and various hydrocarbon complexes. Imaging of these surfaces, brought to us by spacecraft like New Horizons, Cassini, Rosetta and others, reveal complex and often-mysterious geological structures composed of these materials. A major step toward explaining both the observed geology and to establish correct evolutionary timescales on these bodies is to acquire a better understanding and accurate quantification of the material strength and dynamic deformation of these volatile ices. The empirical data gathered is essential for accurate physical modeling of these surfaces using state of the art landform evolution modeling, also done here at NASA-ARC. *A new frontier is to develop this knowledge of these ices in both their pure and alloy forms – that latter of which has not been done before.* Beyond this pure scientific motive, vis-à-vis geology and geologic evolution, the nature of the surface holds clues to the interiors of these bodies. As has been posited by the planetary science community over the last 20 years, many of these worlds harbor subsurface liquid H₂O oceans like Europa's and if life is emergent under such conditions then signs of organic activity/residue/detritus may manifest themselves on the surface – whether or not this is feasible depends a lot on what the material characteristics are of the surface substrate upon which this material would end up. In this sense, then, it is of scientific importance for NASA mission planning to both theoretically understand and quantitatively characterize the mechanical properties of these materials as such knowledge will help inform future NASA Discovery and Orbiter class mission studies to the outer solar system.

To date, however, very little laboratory work has been done toward ascertaining the rheological properties of these volatile ices *and their alloy mixtures* (see below). However, there is a long history of this type of laboratory work done on H₂O ice – across a range of pressures/stresses, in its varied phases and as related hydrates. Durham and Goldsby and co-workers have developed laboratory techniques to study various thermophysical properties of cold water ices including their heat capacity, thermal conductivity, material strength, rheology and grain sizes (see comprehensive review Durham et al., 2010). The interest in the mechanical properties of H₂O ices has been for temperature ranges that are appropriate to the Jovian-Saturnian system (90-300K) and under high differential stresses (>10-100 MPa ↔ 100-1000 atm). For planetary bodies of the outer solar system, interest is directed at characterizing material behavior at lower temperatures and weaker stresses. For example, on Pluto we are often concerned about the mechanical properties of CH₄ at temperatures around 20-60K and under differential stresses ranging from 1-100 KPa (0.01-1 atm). These conditions are also relevant for the whole range of Kuiper Belt and Trans-Neptunian Objects (TNOs) and, as such, it is our goal to examine and characterize the rheologies of these volatile ices under these thermo-mechanical conditions. Running experiments to investigate the properties of volatile ices under these relatively gentle but extremely cold conditions requires commitment and patience: the low strain rates of interest will likely require an experiment to run for anywhere from days to weeks in order to obtain a single data point – these matters are further discussed in the section entitled “Volatile Ice Rheology”. Given the time intense nature to run such experiments, it will be advantageous to have anywhere from 3-5 identical experimental apparatuses setup to run experiments to cover a variety of temperatures and strain rates.

Past work. There are two studies that address the rheology of both N₂ and CH₄. An earlier semi-empirical study (Eleuskewiecz & Stevenson, 1990) examined the diffusional creep (very slow strain rates) of these ices, in their pure forms, based on NMR studies of defect propagation in doped samples of these ices. The derived volatile ice rheology based on ES91's studies have not been verified in the laboratory but have been heavily cited in the literature. A second recent study (1990) by the group headed by Yasuyuki Yamashita's group (Japan Aerospace Exploration Agency) have assessed the rheology of both volatiles using a low temperature compression apparatus described further in the section entitled "Experimental Apparatus". While valuable in demonstrating the weakly plastic nature of these ices, the experiments were limited and run at strain rates that are so high that it is difficult to safely extrapolate their results onto the strain rates expected for the planetary conditions of interest. These issues are further explained in the next section.

VOLATILE ICE RHEOLOGY

From a model standpoint and as pertaining to planetary conditions, we treat blocks of ices as composed of a single large crystal lattices, or as an amorphous ice, or as a polycrystalline ice, being a collection of grains each being mini-crystal lattice blocks with given crystal lattice orientation (see cartoon in Figure 1). In the context of planetary ices, where the scales of interest are fairly large, it is generally assumed that ice complexes are polycrystalline. Generally speaking, a block of polycrystalline ice subject to an amount of applied stress (whether it be compressive, tensile or shear) will respond to this external forcing either by exhibiting ductile flow or brittle failure. Ductile flow occurs when the applied stresses are not too high and results in the deformation (strain) at a rate (strainrate) that depends upon several factors including the temperature (T) of the ice, the size of the grains (d) comprising the block. Under brittle failure, which tends to occur if the applied stress and/or driven strainrates are very high, the specimen will rapidly develop cracks and fissures which spread through the block section and result in structural disintegration. Our interest will focus mainly upon the ductile flow regime of solids – but knowledge of the brittle limits of given ices is also extremely important for understanding volatile ices (discussed further in the next section).

When considering the ductile regime, so-called Newtonian rheology refers to solid-state materials whose strainrates, $\dot{\epsilon}$, linearly depends upon the applied stress, τ (see Figure 1 and its caption for more detail). However, many ices, including H₂O, exhibit strainrates that nonlinearly depend upon the applied stress, and such rheology is termed non-Newtonian. Furthermore, based on previous laboratory analysis and various theoretical considerations, the temperature dependence of the strainrate takes on an Arrhenius form. Under given local laboratory conditions, an ice block's strainrate is characterized by the assumed empirical form (Durham et al., 2010),

$$\dot{\epsilon} = Ad^{-p}\tau^n \exp\left[\frac{T_{act}}{T}\right], \quad (1)$$

where the exponents, p, n , the coefficient, A , and the activation temperature of the Arrhenius dependence, T_{act} , are experimentally determined quantities.

The problem of characterization is subtler than it appears because the response will depend upon which mechanism of deformation is active under the given conditions. In general, a polycrystalline specimen comprised of grains of a particular size will deform by “creep mechanisms” which depend upon the applied stress as well as the temperature. As such, the values of the experimentally determined exponents and activation temperatures will vary as a function of τ and T . Another important matter is best appreciated by referencing Figure 1: it is often the case that the response of an ice block will be different whether a sample is in compression versus tension. Similarly, the strainrate may be different from the compression/tension case versus the sheared case. (A terrestrial example is the formation of crevasses on the surfaces of rapidly expanding glaciers wherein the ice on the glacier’s surface begins to fracture under the intense tensile strainrates it is subject. In this case the tensile stresses exceed the range permissible for ductile flow.)

As written, the empirical relationship in Eq. (1) expresses the stress-strainrate dependence in a general fashion -- see further discussion in Figure. 1 – but it should be kept in mind that it is desirable to directly examine the response of these volatile ices under these differing types of applied stresses. Laboratory experiments done on ices appropriate to planetary surface conditions have exclusively conducted compression experiments – generally extending these results as being appropriate for the two other stress conditions.

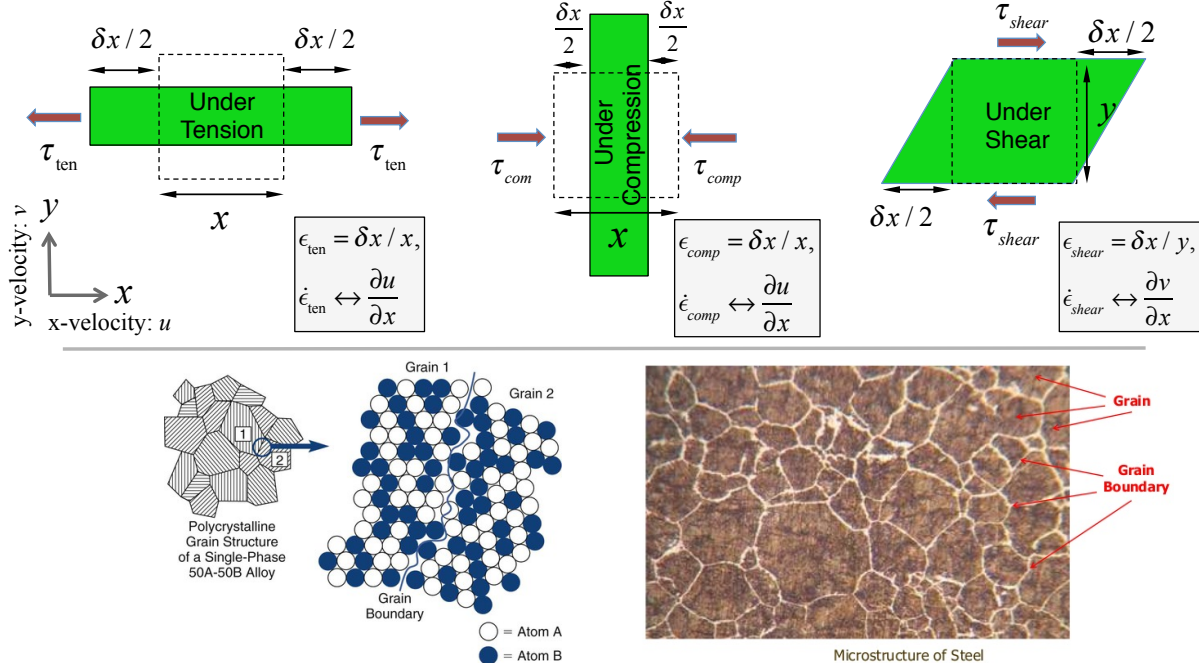


Figure 1. Top row of diagrams illustrate each of the three kinds of stresses possible on a block of ice: tensile, compressive and shear. The corresponding strain ϵ (defined as the differential change in the length of the body divided by the length) is labeled according to the type of stress applied, τ . In general, each type of applied stress will give rise to differing strain deformations – although in modeling considerations they are equated. Strainrates $\dot{\epsilon}$ translate to velocity gradients. Bottom panels illustrate the nature of polycrystalline ices. Each grain will have a preferred symmetry axis but these will vary in orientation from grain to grain. Grain motion will often occur along grain boundaries. The bottom left shows the microstructure of steel.

The types of ice creep mechanisms, which are varied and often interdependent upon one another, can be broadly broken down into grain size sensitive (GSS) “diffusion flow” and grains-size independent (GSI) “plastic flow”. GSS regimes are generally active when the applied stresses are low and they involve several different grain deforming mechanisms including grain boundary sliding, dislocation slip and others (for a full survey see the book by Petrenko and Whitworth, 1999) with stress exponents in the linear or near linear (“superplastic”) regime. In the GSI regime, deformations occur by the process known as *dislocation glide* wherein suitably oriented grains along dislocation boundaries encounter other dislocations resulting in various sliding sections to “climbing over” one another (see bottom middle of Figure 1). The stress exponents in this plastic regime can be in the range of $n=3-5$. The stress-dependent quality of ice deformation (i.e., which mechanisms are active) can result in extreme variations of the resulting strainrate. ***Characterizing this feature of volatile ices (and their alloys) is of singular importance toward reconstructing the histories of icy bodies of the outer solar system.***

Figure 2 qualitatively depicts the complex rheology of solid H₂O (Ice-I). As can be seen from the figure, the strainrate response as a function of applied stress does not fall on a single line in the (logarithmic) plot but, instead, shows significant changes across the range of applied stresses. For example, it would be foolhardy to perform experiments in the easily accessible high-stress laboratory range and then extrapolate these results to predict the strainrates when the stresses are 2-3 orders of magnitude less since the behavior of the materials can drastically change across this range of stresses. ***To reliably assess the rheology of volatile ices requires mapping out and identifying all of the above described response regions – from the dislocation creep regime down to the diffusion regime.***

Developing an accurate empirically derived “equation of state” of these solids is central toward assessing the longevity of structures under various types of applied stress. In the case of H₂O ice in some of its various ice phases and clathrates (especially under conditions appropriate for both terrestrial and Europa conditions), these equations of state are fairly well mapped out (see Figure 3). No such information currently exists for volatile ices under the conditions appropriate for the satellites and solid surfaces of the outer solar system. Figure 3 also usefully identifies stress regions expected for the icy satellites of the Galilean and Saturnian systems. By extension, the conditions for the outer solar system objects will be in the similar ranges of 1-100 kPa. The corresponding predicted strainrates are on the order of 1000’s to billions of Earth years. Thus, the

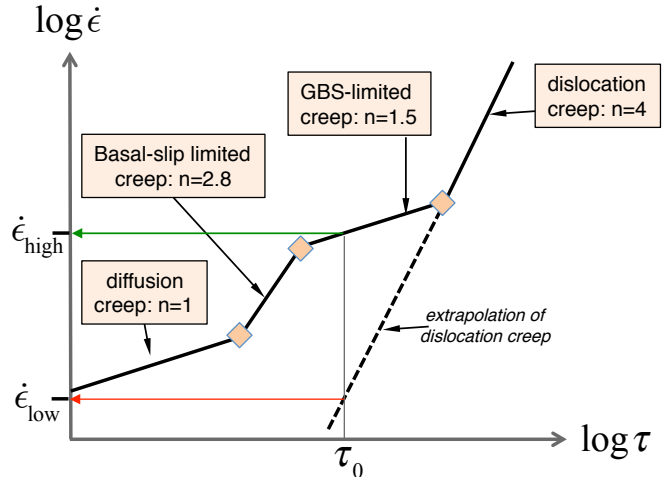


Figure 2. This figure depicts a schematic of the stress-strain rate of H₂O ice (Ice-I) across a range of applied stresses. Figure adapted from Goldsby and Kolstadt (2001). Various flow/creep regimes of H₂O are shown. Lines of extrapolation lines of each of the four creep regions are also shown. There is danger in extrapolating too far in either direction of sampled stress regimes.. For example, if data were available only from the dislocation regime and one wants to know the strainrate for a given stress τ_0 , one would severely underestimate the strainrate based on the extrapolated rheology based on its measured rheology. Peach colored diamonds designate stress values at which creep mechanisms change type. ***To reliably assess the rheology of volatile ices requires mapping out and identifying all of the regions connecting the plastic dislocation creep ($n=4$) regime down to the diffusion ($n=1$) regime.***

predicted evolutionary timescales are intimately tied to the temporal response of a given material under appropriate applied stress. Accurate measurements of their responses will provide reliable estimates for the ages of the variety of ice structures seen on the surfaces of these outer solar system bodies. As such: *these figures are not reliably known for volatile ices existing under the conditions of the outer solar system.*

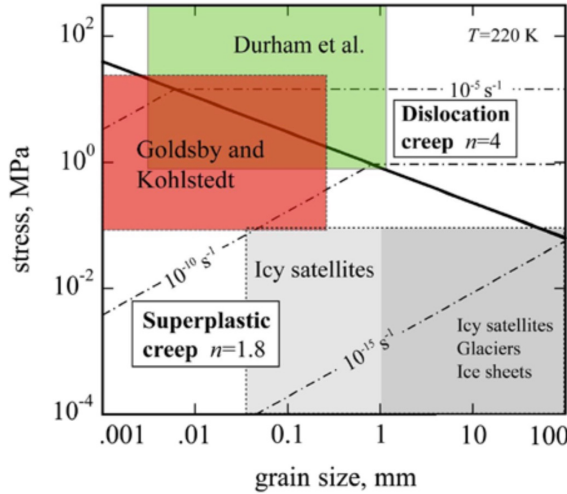


Figure 3. Regimes of H_2O Ice-I examined by various laboratory experiments (authors of studies indicated). The regimes appropriate to the icy satellites are indicated. Values of the strainrates in H_2O ice are extrapolated here. Similar “parameter maps” are needed for volatile ices N_2 , CO and CH_4 , and their alloys, under conditions appropriate for the Kuiper Belt and TNOs.

Our aim will be to construct equally comprehensive assessments of the behavior of pure N_2 , CO and CH_4 ices, as well as their rheological character as alloys. Much in the way steel derives its strength from iron crystals grains interspersed with carbon (up to 20%), we emphasize the central importance of assessing the strengths of analogous kinds of “volatile ice alloys” as geologic formations on places like Pluto (see below) have been spectroscopically determined to be CH_4 dominated composites with a smattering N_2 . As such, the nature and age of high-standing structures like the Bladed Terrain on Pluto depends very much on assessing strength of CH_4 both in its pure and alloyed state.

Laboratory measurements currently available. The work of Yamashita’s group has yielded exponents for pure N_2 and CH_4 ices under very strong stressing (in the vicinity of 0.1 to 10 MPa). Under such conditions the ice response is rapid with strainrates around $10^{-4} - 10^{-6} \text{ s}^{-1}$, i.e., requiring experiments to be run from hours to a week or more. Conditions on the outer solar system bodies (see discussion in the next section) require assessing the strainrate response at far lower stresses, in the range of 1-100 KPa (0.01-1 atm). So far researchers have made predictions regarding the response of both these ices by linearly extrapolating the above response down by several orders of magnitude. Based on our previous reflection, it may be dangerous to do so as one may be wildly over/under-estimating the temporal response given this incomplete information.

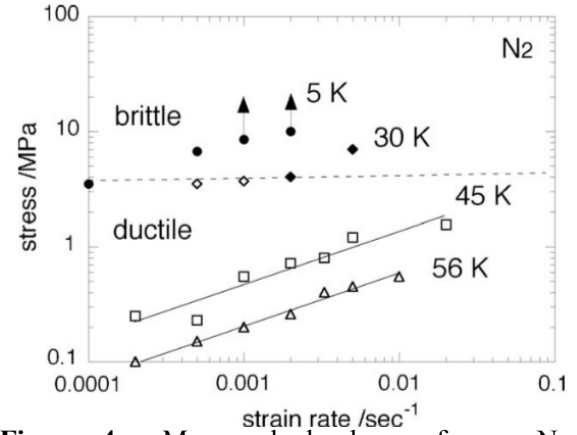


Figure 4. Measured rheology of pure N_2 samples (Yamashita et al., 2010). Two temperature ranges examined. Experiments done in compression. Brittle ductile transition ascertained at around 3 MPa (30 atm).

SOME EXAMPLES FROM AROUND THE OUTER SOLAR SYSTEM

We display a few illustrative example surface features observed on planetary bodies in the outer solar system. The deformation (deviatoric) stresses experienced by a structure (mountain, pits, valleys, etc.) are approximately gauged by estimating both the typical depth of the structure H and the surface elevation slope $\tan\theta$. The basal-stress is estimated by $\tau_b = \rho g H \tan\theta$, where the ice density is ρ and the surface gravity is g .

1. Glacial flow of volatile ices (Pluto). All along the eastern shoreline of Pluto's Sputnik Planitia (surface $g \sim 0.642 \text{ m/s}^2$, during New Horizons flyby: surface $T = 37\text{K}$, surface $P = 1\text{Pa}$) there lies several examples of recent glacial flow from the highlands of Eastern Tombaugh Regio (Figure 5a). On what timescales did this flow occur? Currently this is unknown. The flats of Sputnik Planitia are 2 km below the mean radius of Pluto and they exhibit flow-lobe features indicating the furthest extent of glacial debris deposition. The darkened debris can be traced up into the eastern highlands indicating that the flow originated much higher up and travelled down

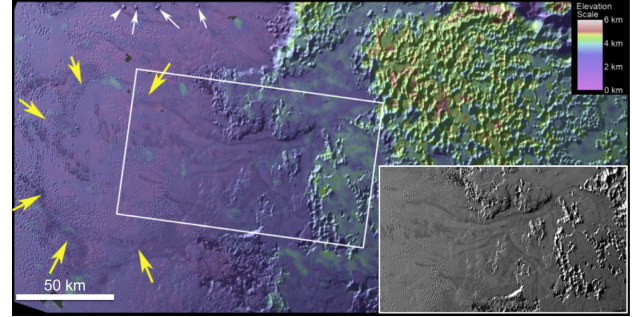


Figure 5a. A section on Pluto displaying evidence of glacial flow. The map shows relative elevation. Inset shows un-doctored figure. Yellow arrows indicate location furthest extent of glacial flow. White arrows indicate possible rafting of H_2O ice blocks. (Umurhan et al., 2017, Howard et al., 2017)

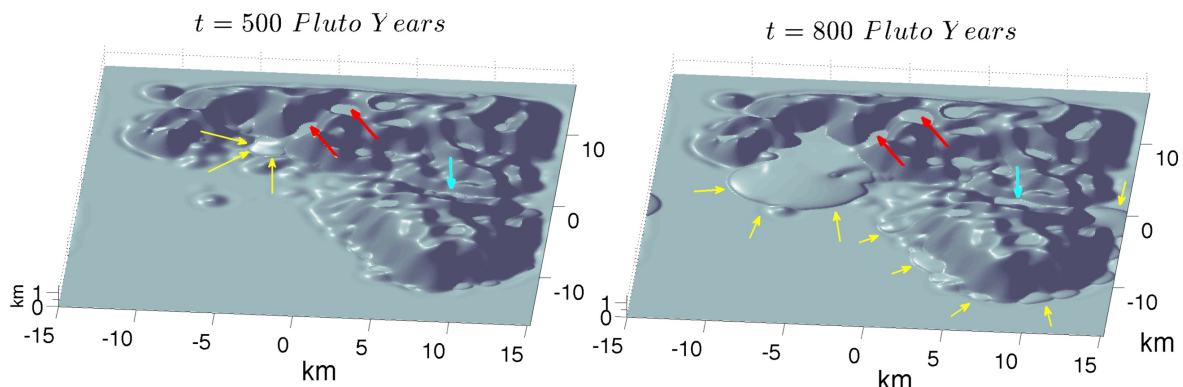


Figure 5b. Simulations of glacial flow on Pluto's surface. Bedrock supports N_2 deposition which is permitted to flow as a N_2 glacier. The N_2 rheology adopted derives from the study of Yamashita et al. (2010). N_2 ice flows and collects in catchments and, after some time, results in drainage at low elevations yielding flow lobe features like shown in Figure 5b. The time scales in which this happens are uncertain due to the uncertain reliability of the rheological experiments done by the Yamashita group.

through several networked channel valleys. These channel valleys, extending 50-100 km in length indicating a typical down-gradient angle of about $\theta \sim 3^\circ - 4^\circ$, are anywhere from 50-400 meters deep. Spectroscopic measurements indicate that Sputnik Planitia contains primarily N_2 ice ($\rho \sim 0.95 \text{ gm/cm}^3$), with a small fraction (5%) of CH_4 ice ($\rho \sim 0.4 \text{ gm/cm}^3$) and trace amounts

(<1%) of CO ice ($\rho \sim 0.95 \text{ gm/cm}^3$), while the highlands of Eastern Tombaugh Regio predominantly contain CH₄ ice with a small smattering of dissolved N₂ ice at similar fractions (Schmitt et al., 2017, Grundy et al., 2016). The corresponding basal stresses experienced on one of these typical channels filled with some kind of N₂-CH₄ mixture (or alloy) is in the range of 1-10 kPa (0.01-0.1 atm). The current laboratory data for either pure N₂ or CH₄ do not extend down to such small stresses. Inferring timescales for drainage based on the laboratory data reported in Yamashita et al.'s study (2010) requires extrapolating past 2-3 orders of magnitude beyond what is reported. Such an estimate based on this data yields a drainage rate on the order 100-1000 Pluto years (e.g. Figure 5b) –the uncertainties in this figure hinges upon the uncertainties in rheology of N₂ ice. *Similar issues pertain to the nature of solid-state convection on Pluto's Sputnik Planitia (not discussed here but of equally important relevance, see McKinnon et al., 2016).*

2. Bladed Terrain (Pluto). East of Pluto's Tombaugh Regio – in regions generally located in a latitudinal band between $\pm 25^\circ$ -- there are methane composed deep structures (500 m) with relatively steep grades $\theta \sim 10^\circ - 20^\circ$ (Figure 6). Never seen anywhere else in the Solar System, the origin of the Bladed Terrain remains a puzzle. Adding to the mystery is the reason why they appear only on parts of Pluto that are at least 1-1.5 km above its mean radius. The structures look like the product of sublimation-shaped processing, much like “penitentes” and “suncups” seen on H₂O ices in very cold and dry climes like the Atacama Desert (Moore et al., 2016, Moores et al., 2017, Moore et al., 2017). With basal deviatoric stresses on the order of 20-50 kPa (0.2-0.5 atm), how long can such a structure survive? The answer to this requires assessing the strainrate of CH₄ under such stresses, either as a pure ice or as an alloy with N₂.

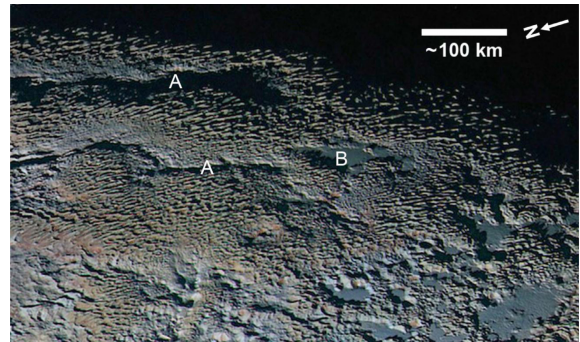


Figure 6. Bladed Terrain on Pluto. Image taken with New Horizons. The patterned CH₄ covered regions are slightly red and showcase elongated ridging often times abutting deep fracture/faults (labeled by A). In various low-lying regions (labeled by B) are smooth patches of N₂ ice.

3. Geysers and Plumes (Triton). Like Pluto, Triton ($T_{\text{surf}} \sim 38 \text{ K}$, $P_{\text{surf}} \sim 1-2 \text{ Pa}$, $g = 0.66 \text{ m/s}^2$) is considered a water world with an H₂O ocean beneath a layer of solid H₂O ice encrusted with a layer of volatile ices (N₂ and CH₄) on its surface. Owing to its retrograde orbit around Neptune, it is currently thought that it is a captured Kuiper Belt object. Being a water world it is an object of interest for future NASA sponsored Discovery class missions. Voyager 2's passage of the Neptunian system in 1989 (before its winter solstice) captured images showcasing features interpreted to be evidence of geysers and plumes. The darkened (low-albedo) plumes forming streak-like features appear to emanate from specific locations of very high albedo surface regions (Figure 7). The darkened materials appear to follow the path of the prevailing winds on Triton. The origins of the geysers remain a mystery and several mechanisms have been proposed (high pressurized water from the H₂O ocean interior to the so-called greenhouse effect). Selecting between either scenario requires knowledge of the brittle strength of the surface volatile ice alloys. For example, the greenhouse effect posits that the relatively high-albedo and sufficiently-transparent volatile ice layer transmits solar irradiance down to several 10's of meters beneath the

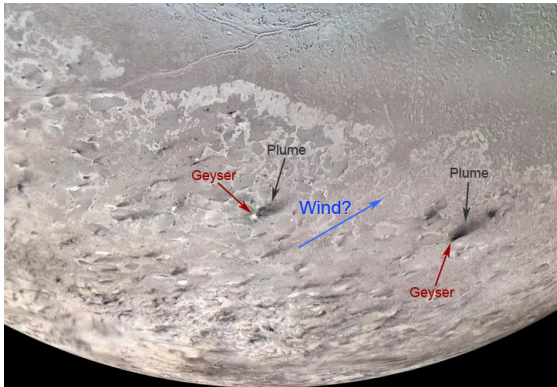


Figure 7. Voyager 2 image of Neptune's moon Triton indicating locations of observed streaks and potential geysers.

surface before being absorbed by a layers/pockets of low-albedo material (perhaps organic molecule contaminated water ice grains intermixed with the same volatile ices). As time goes on, this layer begins to warm-up enough so that solid-gaseous transformation occurs in the volatile pocket. As this continues to heat the pressures begin to rise. At some point the pressure exceeds the bonding strength of the volatile ice layer above – instigating rapid crack formation and the eventual sudden release of the pressurized gases beneath. A relatively low bonding strength would be required to have this scenario plausible. If, on the other hand, the liquid water ocean is the origin of the geysers, then it may very

well imply that the strength of the surface volatile ice is much larger. Beyond the measurements made by the Yamashita group, which focused only on pure volatile ice species, these figures are unknown. In either event, if the sourcing of the streaks is endogenic, then understanding the properties of these ices are tantamount toward understanding if these locations of Triton's surface harbor signs of organic materials emanating from Triton's deep interior.

VIC (VOLATILE ICE CRUSHER): THE PROPOSED EXPERIMENTAL APPARATUS

Ductile rheology of icy materials (as pure species as well as alloys) can be measured under two stress conditions, that is to say, under compression/tension or under shear. The laboratory experiments made by Durham's group of H₂O ice under high pressures were done using a compression-type of experiment. Yamashita's group also approached their rheology experiments using the same type of compression method (see Figure 9). It should be noted, as per the discussion in section Volatile Ice Rheology, that the rheological response of materials depends upon the quality of the stresses involved and it is the vision of this group to build apparatuses that are able *to more thoroughly explore these features of low temperature volatile ices*. The mechanisms at play in compression under low stresses may not be active when under similar low shears – thus identifying these differences is central to accurate characterization of the deformation of these ices and, consequently, reliable age estimates for the surface features seen on these cold planetary bodies. *To date these measurements have not been done -- but are critical for future planetary science research.*

In the following we describe some general details of the experimental methods followed by a more detailed description of our proposed prototype design.

1. Experimental approach and previous design. Past experiments (Goldsby and Kohlstedt, 2001, Yamashita et al., 2010) extracted rheological information from a compression experiment (hereafter “**compression-rig**”). In compression experiments a cylindrical block of given dimensions (like a hockey-puck) is subject to compression at a given stress and the rate at which it compresses is observed. We are guided by the basic design adopted by the Yamashita group as shown in Figure 9. The caption for this figure details the elements of their design. Our proposed design for VIC (The Volatile Ice Crusher), will have significant differences.

Broadly speaking, the measurement philosophy is the following: a block is placed in a temperature-controlled container and compressed by a stepping motor that can apply a stress of the experimenter's choosing or, if desired, compress the specimen at a given rate. In either case, the amount of force/stress applied by the motor is tracked throughout the course of the experiment using a load-cell. The sides of the puck are exposed either to a vacuum in the chamber or is subject to an ambient pressure. In most applications, the chamber is subject to a vacuum.

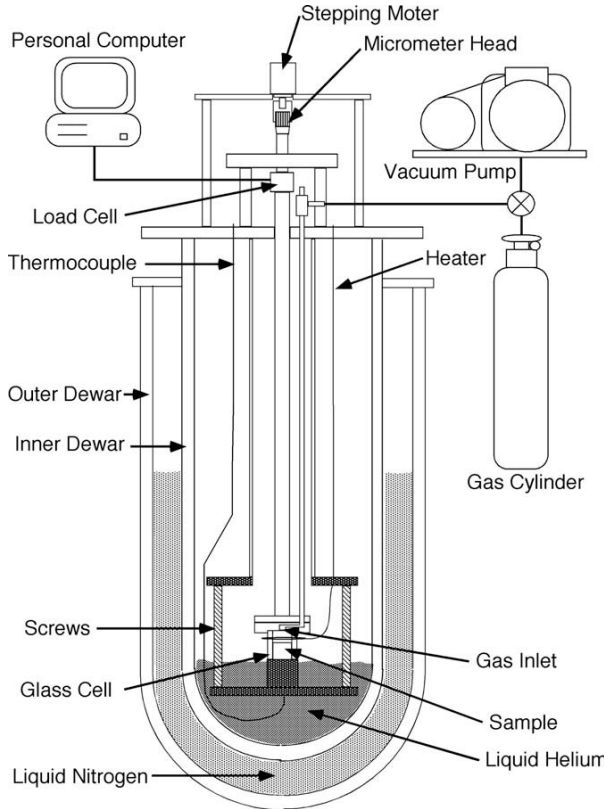


Figure 9. Compression rig design of Yamashita et al. (2010). Outer N₂ dewar jacket thermally shields the inner experimental zone from the ambient terrestrial conditions. The inner region holds liquid He as the main coolant. The crushing chamber is held inside an inner sanctum. The entire interior is held in a vacuum. The sample is grown inside a glass cylinder from spraying gaseous N₂ or CH₄ into the cylinder. Glass cylinder is then slide out and the stepping motor lowers the crushing arm onto the sample which is allowed to expand out sideways. Current design has poor temperature control: in particular, the temperature of the crushing plate is not well monitored or controlled as it is thermally separated from the inner sanctum. This may cause the upper portion of the ice sample to be warmer than reported which could lead to erroneous rheological measurements. On the other hand, the jacketed double-dewar design is one we would implement in our envisioned next-generation design. This design is to be considered against our proposed design shown in Figure 10.

The net applied stress upon the sample is the difference between the compression applied by the load and the ambient pressure on the exposed sides of the sample. A puck with given instantaneous axial length z will shrink at an instantaneous rate of \dot{z} so that at every instant the strainrate, $\dot{\epsilon} = \dot{z} / z$, can be measured. As the sample compresses it expands out along its sides. The vertical shrinking rate can be accurately tracked either using a laser to track the advance of the compressing top lid of the sample or a micrometer that monitors gear advance.

A central challenge is to design an experimental apparatus that (A) better controls the temperature of the ice sample, (B) allows some control of the size of the ice-grains that compose the ice sample, and (C) permits measurement of grain size. In this respect, our prototype design diverges from the apparatus used by the Yamashita group.

Additionally, it is desirable to compare the results of the compressional rig against a shearing rig. *This, too, has yet to been done for low-temperature volatile ices.* As discussed in the section “Volatile Ice Rheology”, the active processes by which blocks of volatile ice deform are likely to

be different depending upon the quality of the applied stress. As such, we propose to have the ability to run a shearing experiment (hereafter referred to as the “*shear-rig*”). In a shearing-rig, the ice sample would be placed within the gap between two concentric cylinders (like a Taylor-Couette experiment) made of metal with relatively high adhesion so the ice is well stuck onto the cylinder walls. The outer cylinder wall would be held fixed while the inner wall would rotate. If funding permits, the shear-rig could be designed as a modular feature wherein the compression motor unit would be modularly switched over to the shearing rig.

In the longer term (3-5 year time frame) we envision at least three rigs to be available for general use, one being the prototype and two being next-generation designs implementing lessons learned from the prototype and folding in desirable features from other rigs like that used by the Yamashita group. With the lessons derived from the construction and operation of the prototype we would seek funding to build to build these next-generation units. In the following we describe our proposed prototype.

2. *Volatile Ice Crusher (VIC)*. VIC is our proposed prototype compression-rig (Figure 10). A large fraction of the apparatus can be assembled from parts already available at NASA-ARC’s Airborne Instrument Design Laboratory (AIDL) located in Building 245. This has certain obvious advantages:

- A. a viable, scientifically productive experimental apparatus can be built onsite,
- B. the construction costs for this prototype will be relatively minimal, and
- C. a tested and calibrated unit will yield new results in under 18 months.

The success of this prototype and the ensuing program will be the basis toward building two of our envisioned next-generation units.

At this prototype stage, the main objectives for VIC’s design is to have a unit that maintains temperature stability and permits the experimenter to both influence and assess the size of grains that form in the ice sample that is “grown”.

VIC will be a vacuum chamber unit holding two dewars. A top dewar will hold liquid N₂ (henceforth, we call this the nitrogen-dewar) while the bottom dewar will hold liquid Ne (i.e., the neon-dewar). Attached to both dewars and passing through a cold plate will be a pipe that delivers a liquid CH₄-N₂ mixture at controlled temperatures.

The neon-dewar will be the primary source of cooling for the ice in the experimental chamber., Neon is liquid in the range of 20-40K at terrestrial pressures. We choose neon to be the primary coolant since it will bring the ice samples down to the temperatures of interest. Neon is also attractive since it is relatively cheap compared to helium. However, some concerns with respect to overall cost of acquiring liquid neon (despite its relative affordability) may force us into considering using a closed circuit cryo-refrigeration unit and design (see end of Section 4).

Nevertheless, under this neon-cooled cold plate and directly attached to it is an experiment chamber. The liquid sample is deposited in the experiment chamber, which is slightly offset to one side of the neon-dewar’s centerline. This asymmetry in the experiment chamber’s position arises

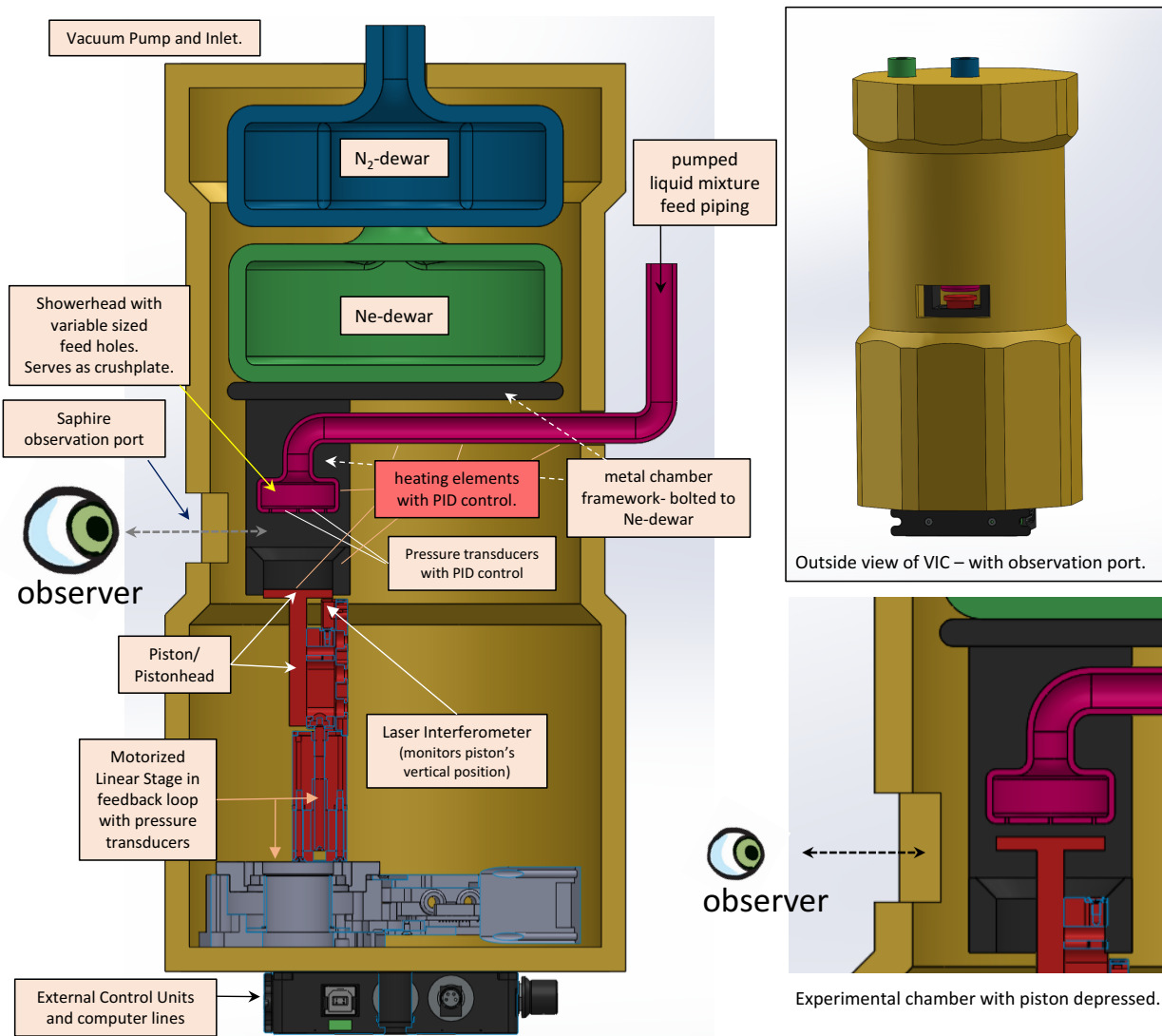


Figure 10. Schematic for VIC (Volatile Ice Crusher). Left panel details elements described in text. Observer indicates position of stereo microscope to assess grain size. Top right shows outside view of unit. Bottom right shows experimental chamber with piston depressed.

from experimental necessities following certain mechanical and optical designs discussed further below. The primary concern will be to get the ice sample as close as possible to the stereo microscope in order to assess the grain sizes in the ice sample.

The liquid sample will be fed through a flat showerhead nozzle (possibly rotating) with several injection ports on the showerhead, with individual porthole diameter sizes that may be mechanically controlled to affect droplet size. The liquid mixture will be dripped into a 25mm cylindrical or square (depending upon final design) bore with a piston floor recessed 10mm from the experiment chamber. The shower line and head will be mounted on the neon-dewar so as to affect the temperature of the metal structure. Several heating elements and thermocouples will be attached along both the feedline, showerhead and bore region in order to precisely control temperature. In this way, the volatile ice sample may be grown with some modicum of control

over the size of grains that are manifest within the block. We will dual-purpose the flat showerhead as the crush plate onto which the ice sample is pressed (see below).

Driving the piston upon which the ice sample sits is a vacuum-rated linear motion stage. Activation of this stage raises the ice sample from out of the collection chamber and into the experiment chamber (see figure). From there, the linear stage may continue its forward motion until the ice sample is compressed against the crush plate. We have found several vendors that have motors that can operate slow enough to reliably measure strainrates of about $\dot{\epsilon} \sim 10^{-6}$ s⁻¹ for ice samples that are 1 cm thick.¹

To assess the applied stresses, we will experiment with two relatively inexpensive approaches. In one, a force gauge between the piston and the linear stage measures the applied stress driving the motor. With appropriate controlled calibration, the amount of stress applied may be monitored. In the other approach, the shower head will have transducers built onto their flat sections which would directly measure the applied stress in situ. We also have contingencies in place to consider a redesign of the injection line system: in-series with the showerhead a separate crush-plate structure is fashioned which can be linearly slotted into place after the ice-sample has been fashioned (this feature is not shown in the Figure 11a/b but will be part of a revised design if necessary).

Built into this part of the experiment will be a feedback mechanism in which the applied stress applied to the sample is maintained within the value of interest. This will be achieved by PID control in which the stress data is fed into a monitoring computer which correspondingly gives commands to change the speed of motion of the linear-stage piston.

Mounted beside the linear-stage/piston unit will be a laser interferometer oriented to monitor the upward progress of the backside of the piston. This will be used to accurately assess the rate of the piston's upward motion. The experiments performed by the Yamashita group were run until the sample had shrunk about 50% of its original axial length. Approaching 50% strains will be time intensive in those experiments where the applied stresses are low. For low applied stresses this will take a lot more time. However, it will be sufficient to capture the transition into an asymptotic strain-rate once the sample has surpassed a minimum strain much less than 0.5 (see further discussion in subsection 4 below). However, with the use of a laser monitor or high precision micrometer, we would not need to be so severely constrained with respect to the total amount strain required to register the data point and this would, in turn, reduce the amount of time spent per datum.

The entire linear-stage/piston unit is mounted on a rotation stage and in a similar process, with a central stationary cylinder in place of the crush plate, the shear forces on the sample may be measured. This will be the modular feature of the unit when we move onto the next-generation design. We mention it here, however, to point out that our prototype design will be done in such a way so as to permit this kind of modularity without having to change any other part of the unit.

¹ Several motors we have found in our searches reliable run with linear speeds of as little as 1×10^{-5} mm/s.

Because this whole part of the experimental unit is offset from the axis of the dewar, it allows for monitoring of the experimental chamber via an optical window in the near sidewall of the dewar. In this way will be able to examine individual grains present in the ice sample and to directly observe the manner in which they are deformed during compression.

On the outside of this window a stereo microscope is mounted allowing the procedure to be recorded and analysis of the shape and deformation of the sample. Such microscopes have a working distance of ~100mm and at 7x magnification give a field of view just big enough to view our sample (~28mm). We also have the capability to zoom in up to 90x with a small (2.2mm) FoV to observe grain structure. If the observed side of the sample is flat, Analysis of the grain distribution in the sample will be facilitated if the sample is in the shape of a rectangular box rather than a cylinder (see above) – this will be decided during the detailed design phase of the effort.

Thermocouples throughout the experiment chamber and sample tube along with cold plates and heating elements allow precise and continuous monitoring and (PID) adjustment of the sample temperature environment. This is a critical feature of our design as temperature control at every stage of the sample formation and subsequent stress testing must be constrained as best as possible.

LED lighting for the microscope observations may be necessary but can be placed behind cold windows. This setup allows the potential to add polarization filters for measurements of polarized light to enhance contrast of ice grains and more detailed optical measurements.

3. Typical Experimental Procedure. By way of illustration we describe the steps toward setting up and running a typical run for testing an alloy mixture of CH₄-N₂ in which N₂ is the minor component (much less than the eutectic fraction of about %75, see Figure 11).

- i. A premixed liquid sample, provided by a vendor, held at a suitable temperature, will be injected into the pipe and delivered under mild pressure to the showerhead.
- ii. The temperature all along the pipe and showerhead will be held at temperatures that maintain the liquid mixture insuring that no freezing (sedimentation) takes place along the line (see red arrows in Figure 11).
 - a. The liquid will be dripped into the collection chamber (the plug region above the piston and between the container walls). The temperature of the chamber walls and piston will be maintained so as to efficiently realize the following:
 - b. By appropriately engaging the heating elements on the structure, the temperature will be lowered to a given fixed value. At this value the mixture will begin to form an N₂ poor CH₄ ice whose N₂ concentration is known from its phase diagram. Because the chamber is in vacuum the part of the mixture that remains liquid will rapidly sublime away leaving the just the ice. Pre-calculated theoretical curves will make an estimate of the remaining relative molecular fraction in the ice sample.
 - c. With the pure ice sample purified of its liquid, the temperature of the apparatus is then steadily lowered down to the temperature of our choice.
 - d. By carefully noting the mass of the input and the load cell measured force required to raise the ice block on the linear stage, an estimate of the relative proportions of the N₂-CH₄ mixture can be measured.

- iii. The piston is raised and the block will come into view of the glass window allowing for periodic (over the course of the experiment) high resolution images to be taken to assess grain size.
- iv. The ice sample carrying piston is raised until the top of block touches the crushing plate and the compression part of the experiment may begin.
- v. At this stage, the long phase of the experiment begins. The laser interferometer and the force transducers will monitor the applied stress and upward piston advance. Because this is a feedback design, the rate of upward advance will always be adjusted to make sure that a constant stress is being applied to the block.
- vi. The strainrate will be monitored on a pre-set basis (depending upon the stresses being examined) and once either 50% strain is achieved or a transition into the asymptotically steady strainrate regime has been observed to have occurred (see next section for this), the experiment is terminated.
- vii. The temperature of the chamber is raised allowing the ice to get evacuated via the process of sublimation.

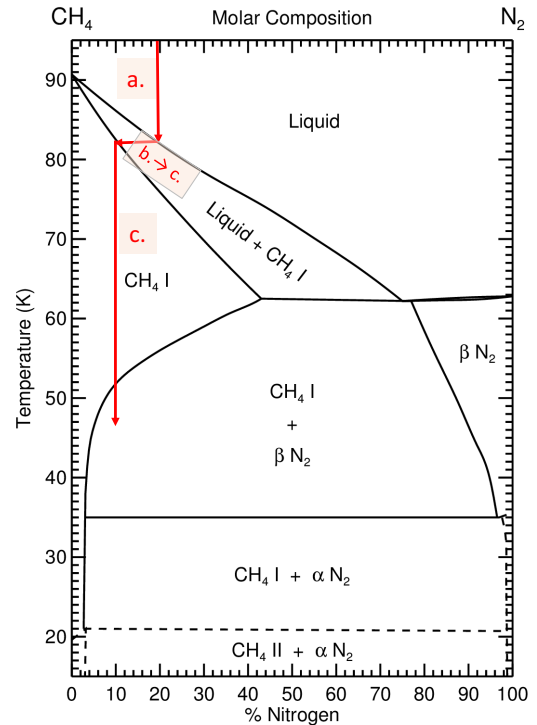


Figure 21. Binary phase diagram for CH₄-N₂. Various stages of the sample assembly process (i.e., the sub-procedures described in step ii.) are indicated by red arrows and letters in graph.

4. Measurements: time estimates and bootstrapping. It is important to make estimates of the time it would take to make single measurements in the compression-rig setup. By way of example, we refer to Figure 4 displaying the results reported by Yamashita et al. (2010) under the high stress regimes for N₂. Their compression experiments were run until the sample was reduced to 50% of its original axial length. By reading-off strainrate values from the graph and estimating the timescale of a given run to be approximately $t_{\text{run}} \approx (\ln 2)/\dot{\epsilon}$, we see that the experiments run at low compressional stresses (0.2 MPa, 2 atm.) took approximately 1.5 hours to run through to completion. Taking rig and sample preparation into account (including the time to clean out the apparatus) means that in order obtain a data point at these stresses could take up to 4-5 hours of lab time.

Our aims are to run these experiments at even lower applied stresses. It is difficult to estimate the time it would take to perform runs at stresses as low as 1-10 kPa for lack of any knowledge of the response of these ices (and their alloys) is under those conditions – it being the primary purpose of this proposed endeavor! For strainrates that are a hundred times slower, i.e., $\dot{\epsilon} \sim 10^{-6} \text{ s}^{-1}$ means running experiments for 100's of hours (approximately a week).

There are some ways around this problem, which requires us to consider the theory of elastic deformation of icy solids. In short, the measured strainrate under constant applied stress will experience a short term rapid response followed by an asymptotic regime once a minimum strain,

ϵ_{\min} , is achieved (Figure 12). The strainrate exhibited once this minimum strain is achieved is the target value. As such, one does not need to run the experiment until samples have shrunk by 50% but instead by values of 10% or less: with a laser constantly monitoring the position of the compressing lid, we can capture the transition into the steady asymptotic strainrate and, thereby, reduce the time needed to run the experiment. Given the above-mentioned example ($\dot{\epsilon} \sim 10^{-6} \text{ s}^{-1}$) if the steady strainrate is achieved after a minimum strain of 10% would mean then the data point would be reliably obtained in about 1 day.

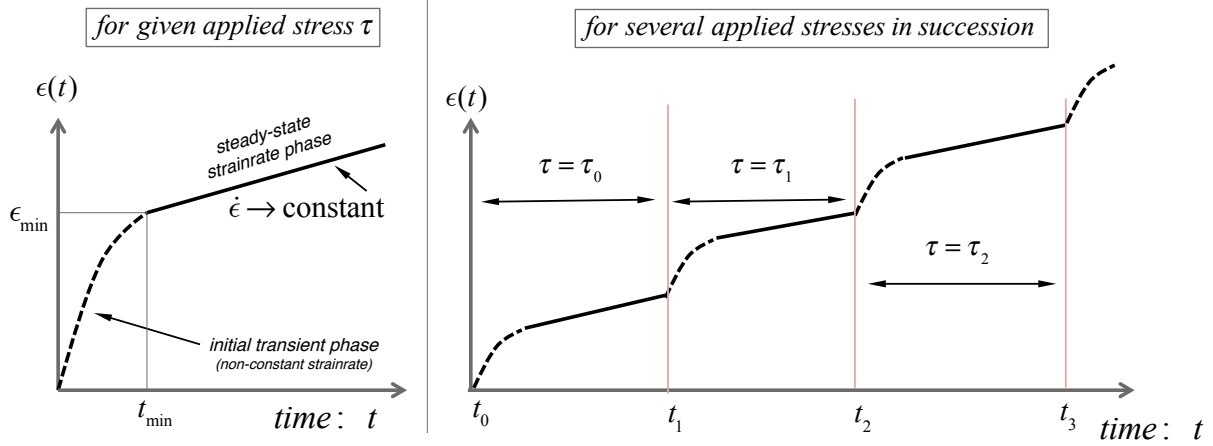


Figure 12. Left panel depicts strain as a function of time for a given applied stress. Initial unsteady strainrate phase is followed by steady state strainrate phase which is the target measurement quantity. Right panel depicts the bootstrapping scheme discussed in text where an applied stress for a given sample is permitted to reach a steady state strainrate whereupon a new stress is applied to the same sample. The process continues. The advantage of this experimental approach is that it minimizes the time spent on preparing new samples for each applied stress. With laser monitoring, the transition into the steady strainrate phase can be assessed without spending too much time in that phase. This facilitates efficient data acquisition.

Another advantage of near continuous laser monitoring is that for sufficiently tall cylindrical (or block) ice samples (2-3 cm in height, maybe larger) one can perform a series of experiments upon the same sample without having to reconfigure the chamber for each value of the applied stress. Note that the prototype will be designed for samples about 1.2 cm in height, so that taller samples will be testable in any new-generation design. Nevertheless, this “bootstrapping tactic” follows once the sample begins to exhibit the steady state strainrate, the stepping motor can be adjusted to a slightly higher applied stress. After the initial transient response under this new stress has subsided (by having the sample cross over its “new” ϵ_{\min}), then a new asymptotic/steady-state strainrate can be recorded and so on². Supposing the minimum strain required for steady-state is indeed 10% and if this proposed bootstrapping approach proves viable, then experimental results, like those of Yamashita et al. (2010) shown in Figure 3, could be reproduced in as little as 1 day. Coupled with steady laser monitoring, this bootstrapping method would then make it possible to reliably make measurements at lower stresses with enhanced data acquisition efficiency.

² This tack is often adopted in numerical experiments of turbulence (e.g., Lesur and Longaretti, 2005).

Extended Use. One of the limitations of the design is that the Ne-dewar has only a single pass into its chamber. Because neon will be the primary coolant of the experimental chamber of the apparatus, over time the neon will boil off. Excessive boil-off of this coolant means added costs in terms of purchasing replacement neon. We have opted for neon because of its relative cheapness compared to helium, but long-term usage will result in increasing costs since it is still an order of magnitude more expensive than liquid N₂. While we do not expect this will not be a serious problem for short term runs (a few hours to half days at a time), for runs that are much longer in duration (on the order of days to weeks) the increasing costs arising from replenishing neon may force us to reconsider a redesign of the prototype to make it conformable with a closed-circuit cryo-refrigeration unit. The long-term advantage of this is that the amount of neon is conserved and little or no extra costs will go to buying new liquid neon. However, the obvious disadvantage comes from the perspective of initial cost: such closed-circuit refrigeration units run between \$30-\$50K (see Appendix A). In any event, a next-generation design will be drawn up to include this coolant recycling feature.

2-5-8-10 YEAR GOALS

2 Year Goals.

1. *Purchase equipment, design and build compression experiment prototype and reproduce Yamashita et al. (2010)'s series of experiments as well as new never done before CH₄-N₂ alloy experiments. (first 18 months).*
2. Repeat some selected low-stress H₂O experiments reported in Durham et al. (2010) to establish calibration and validate robustness of experimental design.
3. Reproduce measurements of pure volatile ices (N₂ and CH₄) made by Yamashita's group. Verify brittle-ductile transition regimes. Demonstrate viability of bootstrapping measurement technique.
4. Perform one set of CH₄-N₂ alloy experiments.
5. First round of papers and presentation at several conferences (AAS-DPS, LPSC, AGU).
6. Begin advertising NASA-ARC as the facility in the USA that does these kinds of rheology experiments.

5 Year Goals.

7. Develop methods to better control the size of grains appearing in ice samples.
8. Design and build two next-generation rigs. One as compression and one as shear **or** have two generally purpose apparatuses build with the type of experiment to be performed as modular (see above).
9. Perform several low stress experiments of pure volatiles (CO, CH₄ and N₂). 1 apparatus purely committed to this activity. Determine differences in ice response between shear and compressional stresses.
10. Begin detailed examination of CO rheology.
11. Examine full parameter space of various CH₄ and N₂ alloy mixtures. Initially these are done at relatively high stresses (high strainrates, short completion times using the bootstrapping method).

12. Have NASA-ARC's Ice Rheology Lab ready and open to the community at large to perform other kinds of ice experiments.

8 Year Goals.

13. Have a thorough characterization of the rheology response of N₂ and CH₄ in the pure and varied alloy forms accurate down to stresses of 10 kPa for a variety of polycrystalline ice grain sizes.
14. Begin work on rheological information of N₂-CO alloys.
15. Develop theory to support discovered features and write and present results to the community at large.
16. Commence trinary (N₂ - CH₄ – CO) alloy studies.

10 Year Goals.

14. CH₄ clathrate experiments
15. Continue trinary alloy experiments

PROPOSED COSTS OF A PROTOTYPE AND PERSONNEL ROLES

This section summarizes the costs to build, test and generate a first round of publishable results all in the span of **18 months**. The total cost of the effort, including equipment and man-hours is in the vicinity of **\$325,000**. A higher figure in the vicinity of **\$400,000** would be incurred if the fabrication of a long-use unit is preferred.

The prototype will follow the basic design described in the previous sections and its construction will be carried out at NASA-ARC's Airborne Instrument Design Laboratory (AIDL). ***This in-house facility is an ideal choice given their years of experience in fabricating low temperature instruments like NASA-ARC's CUBE-sat.***

Table 1 contains a cost estimate to build a single prototype compression-rig. A detailed cost estimate is shown in Appendix A. Table 2 presents a timeline for the above described 18 months of activity: The proposed time of fabrication, calibration and testing is estimated to take 10-12 months, the first round of data acquisition and preparation of results for publication and socialization (conferences) is expected to be in the range of 6-8 months.

All costs include labor and materials. The costs summarized in Table 1 shows the high-end cost while the Appendix A expresses both a high and a low-end figure. The low-end figure shown in Appendix A (~\$290K) reflects the availability of many of the components needed construct the instrument in AIDL. The high-end figure (~\$325K) assumes all materials are purchased new. Given the availability of much of the parts at AMES-ARC, we expect the lower figure to be the likely cost.

In all cases, the final cost figure is dominated by FTE's and contractor salaries.

Prototype Effort Cost Summary				
Civil Servant Labor	Test, Fabrication, Project Oversight (Codes S & R)	0.5	FTE	12 mo.
Contract Labor	Science, engineering (Codes S & R)	257	K\$	17-18 mo.
Materials Costs	Prototype only	66	K\$	
Materials Costs (alt)	Prototype – extended use with cryopump	146	K\$	
TOTAL non-CS costs	Prototype only with new parts	323	K\$	
TOTAL non-CS costs - II	Prototype only with recycled parts	290	K\$	
TOTAL non-CS costs (alt)	Prototype (new parts) & as extended use	403	K\$	

Table 1

Task	Month #																	TOTALS
	1	2	3	4	5	6	7	8	9	10	11	12	13	14	15	16	17	
Refurbish large dewar - design & modify optical port, electrical & mechanical passthroughs	1.00	1.00	1.00															
Provide design input	0.20	0.20	0.20															
Select long lead items		0.20	0.13	0.10														
Purchase long lead items		0.10	0.10	0.10														
Cut windows for microscope, manufacture dewar extension				0.50	0.50													
Assemble, Test and calibrate vacuum seal, electrical connections, optics, and thermal control					0.80	0.75	0.50											
Experiment with water ice (Durham)							1.25	1.25	1.25	1.25	1.25							
Troubleshoot prototype, make small modifications								0.75	0.50	0.25	0.20							
Experiment with Pure N2, pure Methane (Yamashita et al)													1.25	1.15	1.00			
Test bootstrapping process																1.50	1.50	
Total FTE's & WYE's /month	1.20	1.50	1.43	0.70	1.30	0.75	1.75	1.25	2.00	1.75	1.50	0.20	1.25	1.15	1.00	1.50	1.50	1.28
Approximate FTE's (CS hours)	0.50	0.60	0.60	0.60	1.00	0.50	0.50	-	0.50	0.50	0.20	0.10						0.47
Approximate \$\$ (Contractor, Student)	11,156	14,344	13,148	1,594	4,781	3,984	19,922	19,922	23,906	19,922	20,719	1,594	19,922	18,328	15,938	23,906	23,906	256,992

93.75 Combined Rate

	Science work
	Engineering work

Table 2

The alternative cost estimate shown in the last line of Table 2 reflects the construction of a prototype with extended use capabilities (see discussion in subsection 4 of “Experimental Apparatus”). This extended use capability includes the cost of repurposing the Ne-dewar to support a second input/output valve in order for it to be attached to a low temperature cryopump. This is a relatively expensive piece of equipment but it will cut down on aggregate costs involved with continual resupply of liquid Ne into the Ne-dewar. A cost-benefit analysis would be done once the thermal behavior of the prototype has been assessed.

Dr. Jeffrey Moore has agreed to make available his laboratory space in Building 244 for the working prototype.

The proposed costs presented in Table 1 and the timeline in Table 2 has been reviewed by Andrea Nazzal (Logistics Lead, Millennium Engineering) who finds the cost estimates to be reasonable. In this kind of capacity, Andrea has consulted with previous projects at NASA-ARC including NASA Ames’ CubeSat program (Tony Ricco, Stanford University).

The major actors during the construction and testing phase of this project are detailed below. They have all participated directly in the preparation of all elements found in this document including the initial proposed design shown in Figure 10.

- **Mr. Emmett Quigley** (ARC-SST) will be the lead fabricator of the instrument (ARC-AIDL).
- **Dr. Arwen I. Dave** (Millennium Engineering) will be the engineering design lead and will assist in fabrication.
- **Dr. Orkan Umurhan** (SETI Institute, science lead) will participate in proposing and setting up calibration experiments as well as participate at every stage in the design and fabrication stage of the prototype.
- **Dr. J.M. Moore** (ARC-SST) will oversee the scientific effort and assist in preparing of manuscripts and help with outreach to the other NASA facilities and the larger national level scientific community.
- **Dr. Nicholas Scott** (ARC-SST), will help advise and participate in the design of device properties pertaining to porthole construction and stereo microscope observations, line temperature



Figure 13 The VIC Team: (From left to right): Ms. Chavez, Dr. Dave, Dr. Umurhan, Dr. Scott, Mr. Rogers, Mr. Quiggle. Dr. Moore is not shown.

- control and laser interferometry (0.25 FTE's requested).
- **Ms. Carrie Chavez** (ARC-SST), will participate during the latter stages when the prototype is built by helping to run/monitor the progress of experiments. She will also assist Dr. Umurhan in all aspects of public outreach, document preparation and materials procurement.
- **Mr. Bryce Rogers** (ARC-SST), will participate in CAD design and actual fabrication of prototype as Mr. Quigley's apprentice assistant.

REFERENCES:

- Durham, W.B., Prieto-Ballesteros, O., Goldsby, D.L., J. S. Kargel (2010) Rheological and Thermal Properties of Icy Materials. *Space Sci Rev* 153, 1-4, 273.
<https://doi.org/10.1007/s11214-009-9619-1>.
- Eleskiewicz, J., and D.J. Stevenson (1990) Rheology of solid methane and nitrogen: applications to TRITON. *GRL* 17, 10, 1753.
- Goldsby, D.L. and Kohlstedt, D.L. (2001) Superplastic deformation of ice: Experimental observations, *JGR, Solid Earth* 106, B6, DOI: 10.1029/2000JB900336.
- Grundy, W.M., et al. (2016) Surface compositions across Pluto and Charon, *Science* 351, 6279, DOI: 10.1126/science.aad9189.
- Howard, A.D., et al. (2017) Present and past glaciation on Pluto, *Icarus* 287, 287-300, doi: 10.1016/j.icarus.2016.07.006.
- Lesur, G. and Longaretti, P.-Y. (2005) On the relevance of subcritical hydrodynamic turbulence to accretion disk transport. *A&A* 444, 25.
- McKinnon, et al. (2017) Convection in a volatile nitrogen-ice-rich layer drives Pluto's geological vigour. *Nature* 534, 82–85, doi:10.1038/nature18289
- Moore, J.M., et al. (2016) The geology of Pluto and Charon through the eyes of New Horizons, *Science* 351, aad7055, 1284-1293, doi: 10.1126/science.aad7055.
- Moore, J.M., et al. (2018) Bladed terrain on Pluto: Possible origins and evolution, *Icarus* 300, 129–144.
- Petrenko, V.F. and Whitworth, R.W. (1999) *The Physics of Ice*, Oxford University Press, NY.
- Schmitt, B., et al. (2017) Physical state and distribution of materials at the surface of Pluto from New Horizons LEISA imaging spectrometer, *Icarus* 287, 229-260.
- Umurhan, O.M., et al. (2017) Glacial flow on and onto Pluto's Sputnik Planitia. *Icarus* 287, 301-319.
- Yamashita, Y., M. Kato, M. Arakawa (2010) Experimental study on the rheological properties of polycrystalline solid nitrogen and methane: Implications for tectonic processes on Triton. *Icarus* 207, 972-977, doi: 10.1016/j.icarus.2009.11.032

APPENDIX: A DETAILED LIST OF ESTIMATED MATERIAL/LABOR COSTS

Civil Servant Labor Role	Name	Code	Hours	FTE
LN2 test support	EELV staff / Lynn Hofland	R	20	0
Fabrication	Code S shop / Emmett Quigley	S	1,000	1
Project Oversight	Jeff Moore / Michael Bicay	S	10	0
Ice SME's	Various	S	20	0
Contract Labor Role	Name	Contract	Hours	Dollars (K\$)
Science Lead	Orkan Umurhan	SETI	1,000	100
Student Assistant	TBD		1,000	75
Engineering Support	Arwen Davé	MEI	700	63
Cryo SME's	Nic Scott, Various	R and S	190	19
TOTAL				257
Materials Costs	Item	Use	Cost (\$) Max	Cost (\$) Min
1	Cryopumps (there is a repair place 2 exits up the freeway)	prototype	20,000	some in N246 – can be rebuilt
2	Motor stages	prototype	3,000	2,000
3	Two dewar parts: Liquid nitrogen first, then liquid helium or neon	prototype	N/A	modify existing
4	Height extension machined by Emmett - materials cost	prototype	500	500
5	Laser interferometer to measure deformation	prototype	10,000	3,000
6	light microscope	prototype	5,000	3,000
7	Ultrasonic transducer	prototype	5,000	5,000
8	Gas regulator with cylinder	prototype	300	100
9	Vacuum pump (scroll pump may be needed – oil-free, same pressure)	prototype	5,000	2,000
10	Thermocouples (Au + 0.07%Fe-chromel)	prototype	400	100
11	Multimeter to read the thermocouple	prototype	200	use existing
12	Pressure Transducers	prototype	900	900
13	Passthrough purchase and welding	prototype	2,000	2,000
14	Load cell	prototype	2,000	1,000
15	Glass cell (sapphire cylinder)	prototype	500	370
16	Heater – cartridge to control temperature, or heater wire	prototype	100	100
17	Liquid helium (\$5.20/100 grams)	prototype	9,841	9,841
18	Liquid neon (\$16.00/gallom)	prototype	800	800
19	Liquid nitrogen (50¢/gallon)	prototype	25	use N242 supply
20	Sapphire window or rod	prototype	370	370
21	PID controller (control temperature) = Computer interface for thermocouple (reads voltage and converts to pressure)	prototype	100	46
22	<i>machined parts</i>	<i>permanent</i>	<i>10,000</i>	
23	<i>custom passthroughs for extended use</i>	<i>permanent</i>	<i>20,000</i>	
24	<i>Janis 4K closed cycle refrigerator</i>	<i>permanent</i>	<i>50,000</i>	
TOTAL	Not including items #22-24		66,036	31,127